Sparsity-based blind deconvolution of neural activation signal in fMRI

Hamza Cherkaoui, Thomas Moreau, Abderrahim Halimi, Philippe Ciuciu

SPARSITY-BASED BLIND DECONVOLUTION OF NEURAL ACTIVATION SIGNAL IN FMRI

Hamza Cherkaoui[1,2] *Thomas Moreau*[2] *Abderrahim Halimi*[3] *and* *Philippe Ciuciu*[1,2]

[1]CEA/NeuroSpin, Univ. Paris-Saclay, F-91191 Gif-sur-Yvette, France.
[2] Parietal Team, INRIA Saclay, Université Paris-Saclay, Saclay, France.
[3] School of Engineering and Physical Sciences, Heriot-Watt University, Edinburgh UK.

ABSTRACT

The estimation of the hemodynamic response function (HRF) in functional magnetic resonance imaging (fMRI) is critical to deconvolve a time-resolved neural activity and get insights on the underlying cognitive processes. Existing methods propose to estimate the HRF using the experimental paradigm (EP) in task fMRI as a surrogate of neural activity. These approaches induce a bias as they do not account for latencies in the cognitive responses compared to EP and cannot be applied to resting-state data as no EP is available. In this work, we formulate the joint estimation of the HRF and neural activation signal as a *semi blind deconvolution* problem. Its solution can be approximated using an efficient alternate minimization algorithm. The proposed approach is applied to task fMRI data for validation purpose and compared to a state-of-the-art HRF estimation technique. Numerical experiments suggest that our approach is competitive with others while not requiring EP information.

Index Terms— BOLD signal, Hemodynamic response function (HRF), non-convex optimization.

1. INTRODUCTION

Context. Functional magnetic resonance imaging (fMRI) non-invasively records brain activity by dynamically measuring the blood oxygenation level-dependent (BOLD) contrast. The latter reflects the local changes in the deoxyhemoglobin concentration in the brain [1] and thus indirectly measures neural activity through the neurovascular coupling. This coupling is usually characterized as a linear and time-invariant system and thus summarized by its impulse response, the so called hemodynamic response function (HRF) [2, 3]. Its estimation links the observed signal to the underlying neural activity, which can in turn be used to understand cognitive processes in the healthy brain or to predict neurological diseases.

Related works. Several methods have been designed to estimate this evoked response in the case of task-related fMRI (tfMRI) [4–9]. In this setup, the participant is engaged in an experimental paradigm (EP) during the imaging session, which alternates between one or multiple tasks and rest periods [6, 9–11]. Commonly, supervised HRF estimation methods fit a model to explain the observed BOLD signal from the EP [4, 6–9, 11]. A limitation of these approaches is that the EP is used as a surrogate for the neural activity. Therefore they do not account for possible latencies in the subject's responses compared to the task onsets, thus yielding a biased HRF estimate. Moreover, these methods cannot be used on resting-state fMRI data (rfMRI), where the participant is laying still in the MRI scanner. In this context, no EP is available to serve as neural activity surrogate. Some recent work proposes to estimate such a surrogate by estimating a block signal using a fixed HRF [12]. In doing so, the recovered neural activity signal is used to define functional networks in which the population of neurons have been activated together at the same time. However, as the HRF is not allowed to vary across brain regions, this method potentially produces a biased estimate of the deconvolved neural activity signal.

Goals and contributions. Following the ideas developed in the dictionary learning literature [13], we propose, for each BOLD time series, namely each voxel, to jointly estimate the neural activation signal and the HRF with properly selected constraints. The resulting optimization problem is non-convex but an approximated solution can be computed using alternate minimization, and we propose efficient procedures to perform each step. This algorithm aims at reducing the bias introduced with arbitrarily fixed HRF or EP, by learning the HRF for each voxel and a neural activity signal that can fluctuate and depart from the EP. Unlike previous contributions [14, 15] to make the inversion well-posed, we regularize the neural activity signature with a sparse prior on the first-order derivative and the HRF is parameterized by a single unknow scalar. On real task fMRI datasets, we show that we are able to recover similar effects to state-of-the-art HRF estimation approaches without the knowledge of the EP.

In the following, Section 2 introduces our model for the BOLD signal and our algorithm to estimate the HRF. Then, our technique is evaluated against state-of-the-art algorithm in Section 3. Conclusions and future work are discussed in Section 4.

2. HRF ESTIMATION WITH NEURAL ACTIVATION SPARSE MODEL

In this section, we present our modeling of the BOLD signal and derive an efficient algorithm to estimate its parameters.

Notation. A scalar signal is denoted $x(t)$ and a vector in $\mathbb{R}$ is denoted with a bold case letter $\boldsymbol{x}$. $\boldsymbol{D} \in \mathbb{R}^{n\times n}$ refers to the modified first-order differences operator and $\boldsymbol{L} \in \mathbb{R}^{n\times n}$ to the discrete integration operator:

$$\boldsymbol{D} = \begin{bmatrix} 1 & 0 & \dots & & \\ 1 & -1 & 0 & \dots & \\ 0 & \ddots & \ddots & \ddots & \dots \\ \vdots & \ddots & 0 & 1 & -1 \end{bmatrix}, \boldsymbol{L} = \begin{bmatrix} 1 & 0 & \dots & & \\ 1 & 1 & 0 & \dots & \\ 1 & 1 & 1 & 0 & \dots \\ \vdots & \ddots & \ddots & \ddots & \ddots \end{bmatrix}.$$

2.1. Linear and time-invariant modeling

A common model for the voxelwise BOLD signal $y(t)$ is the linear and time-invariant model (LTI) [3], where the signal is considered as the result of the convolution of a neural activation signal, denoted $z(t)$, with an HRF, here denoted $h(t)$: $y(t) = h(t) \star z(t) + \epsilon(t)$ where $\epsilon(t)$ is an additive noise term. Typically, the HRF $h(t)$ has a restricted support in time and quantifies the neurovascular coupling in a specific brain region. The activation signal $z(t)$ captures the periods during which this particular region is involved in task performance. In practice fMRI data are collected at a discrete sampling rate, called the time of repetition (TR), which typically varies between 1 and 2 s. Vector $\boldsymbol{y} \in \mathbb{R}^n$ thus refers to the BOLD signal measured in each voxel of the brain along n consecutive scans. The discretized LTI model reads: $\boldsymbol{y} = \boldsymbol{h} \star \boldsymbol{z} + \boldsymbol{\epsilon}$ with $\boldsymbol{z}, \boldsymbol{\epsilon} \in \mathbb{R}^n$ and $\boldsymbol{h} \in \mathbb{R}^m$, m being the number of time-points for the HRF, typically smaller than n and spanning over about 20 s. In task fMRI data, the activation signal is usually represented by the piecewise constant time course associated with the experimental design. A common way to enforce such structure in $\boldsymbol{z}$ is to consider its first derivative $\boldsymbol{u} = \boldsymbol{D}\boldsymbol{z}$ to be sparse. To make the computations easier, we inject this prior information in the LTI model and re-parameterize it using $\boldsymbol{u}$ and $\boldsymbol{z} = \boldsymbol{L}\boldsymbol{u}$:

$$\boldsymbol{y} = \boldsymbol{h} \star \boldsymbol{L}\boldsymbol{u} + \boldsymbol{\epsilon}\,. \tag{1}$$

To constrain $\boldsymbol{h}$ to be physiologically plausible, we choose to restrict our model to parametric HRF shapes $\boldsymbol{h_\alpha}$. A classical choice is to select $\boldsymbol{h_\alpha}$ as a the linear combination of d atoms $\sum_{i=1}^{d} \alpha_i \boldsymbol{b_i}$, where $(\boldsymbol{b_i})_{i\in[1..d]}$ are some well define HRF atoms [9, 11, 16]. Here instead, we propose to use a reference HRF denoted h_{ref} [16] and dilate the time such as $\boldsymbol{h}_\alpha$ is the discretization of $h_\alpha(t) = h_{\text{ref}}(\alpha t)$. The main advantage of this choice is to vary the full width at half-maximum (FWHM) of the HRF and its time-to-peak (TP) with only one parameter. The model in Eq. (1) has an ambiguity in magnitude, as if $\boldsymbol{h}$ is multiplied by β and $\boldsymbol{z}$ is scaled down by the same factor, our model remains the same. To fix this scale ambiguity, we set $\|h_{\text{ref}}\|_\infty = 1$.

Algorithm 1: Semi-blind deconvolution scheme of the BOLD signal.

Input: BOLD signal $\boldsymbol{y}$, stopping rule ν

initialization: $\alpha^{(0)}$, $\boldsymbol{u}^{(0)} = 0$, $k = 1$;

repeat

  Deconvolution of the BOLD signal for $\boldsymbol{h}_{\alpha^{(k-1)}}$:

$$\boldsymbol{u}^{(k)} = \underset{\boldsymbol{u}\in\mathbb{R}^n}{\operatorname{argmin}} \frac{1}{2} \|\boldsymbol{h}_{\alpha^{(k-1)}} \star \boldsymbol{L}\boldsymbol{u} - \boldsymbol{y}\|_2^2 + \lambda\|\boldsymbol{u}\|_1$$

  Estimate the HRF parameter with fixed $\boldsymbol{u}^{(k)}$:

$$\alpha^{(k)} = \underset{\alpha\in\mathbb{R}}{\operatorname{argmin}} \frac{1}{2} \left\|\boldsymbol{h}_\alpha \star \boldsymbol{L}\boldsymbol{u}^{(k)} - \boldsymbol{y}\right\|_2^2 \quad \text{subject to } \alpha_{\min} \leqslant \alpha \leqslant \alpha_{\max}$$

until $\|\alpha^{(k)} - \alpha^{(k-1)}\|_2 / \|\alpha^{(k)}\|_2 < \nu$;

2.2. Semi-blind-deconvolution as a joint optimization problem

If the additive noise in Eq. (1) is considered to be Gaussian, the parameter of the HRF α and the derivative of the neural activation signal $\boldsymbol{u}$ can be jointly estimated by solving

$$\begin{aligned} &\underset{\alpha\in\mathbb{R},\boldsymbol{u}\in\mathbb{R}^n}{\operatorname{argmin}} \frac{1}{2} \|\boldsymbol{h}_\alpha \star \boldsymbol{L}\boldsymbol{u} - \boldsymbol{y}\|_2^2 + \lambda\|\boldsymbol{u}\|_1\,, \\ &\text{subject to} \quad \alpha_{\min} \leqslant \alpha \leqslant \alpha_{\max}\,. \end{aligned} \tag{2}$$

This optimization problem is not jointly convex in α and $\boldsymbol{u}$. For a fixed α, it is convex in $\boldsymbol{u}$ and for a fixed $\boldsymbol{u}$, convexity in α is not guaranteed as it depends on the analytical model of $\boldsymbol{h}_{\text{ref}}$. However, this 1-dimensional optimization problem can be solved easily as α is constrained to lie in $[\alpha_{\min}, \alpha_{\max}]$. We minimize Eq. (2) using a block-coordinate descent approach, where we alternate the minimization between $\boldsymbol{u}$ and α. Algorithm 1 details the steps of this procedure.

For the estimation of $\boldsymbol{u}$ with fixed α, the accelerated proximal gradient descent algorithm [17] was used as it provides fast convergence to the optimal solution. Other algorithms such as coordinate descent methods [18, 19], can also be considered. However they do not improve the results as the problem is convex and can only speed up the convergence. For updating α, we resorted to the limited memory BFGS algorithm [20] implemented in [21]. We early-stopped the main loop and each sub-problem too once the iterates stabilized themselves. In practice less than 50 iterations of the main loop were needed to converge. Owing to the global non-convexity, this approach converges to a local minimizer of Eq. (2), which may be suboptimal for our semi-blind deconvolution objective. To limit the impact of the initialization selection, we tested multiple random initializations. However, we found experimentally that initializing α to $\alpha_{\max}$ – i.e. initializing $\boldsymbol{h}_\alpha$ to the HRF with the tighter FWHM – and $\boldsymbol{z}$ to 0 is enough

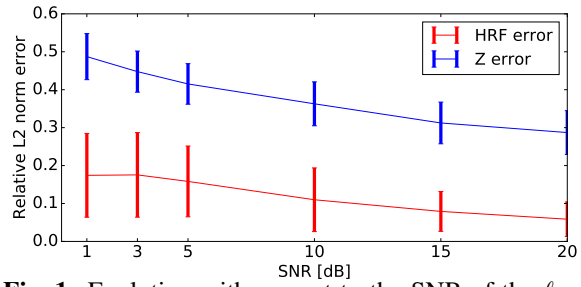

Fig. 1: Evolution with respect to the SNR of the ℓ_2 relative error defined as the mean across voxels of $\|\widehat{\boldsymbol{z}} - \boldsymbol{z}^*\|_2 / \|\boldsymbol{z}^*\|$ for the neural activation signal and as $\|\boldsymbol{h}_{\widehat{\alpha}} - \boldsymbol{h}^*\|_2 / \|\boldsymbol{h}^*\|_2$ for the HRF.

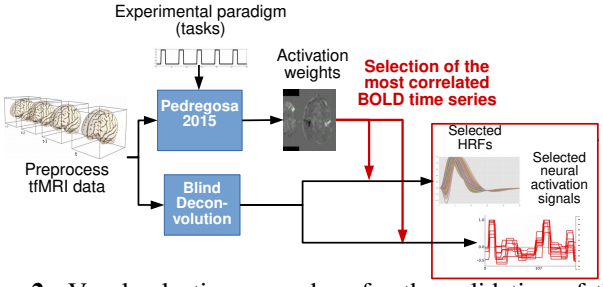

Fig. 2: Voxel selection procedure for the validation of the semi-blind deconvolution method on HCP data. The voxels are selected based on their correlation level with the EP.

to ensure the convergence to reliable estimates. Multiple random initializations on α did not improve the quality of the solution.

3. NUMERICAL EXPERIMENTS

In this section, we validated our approach both on simulated and real task fMRI data. They were collected during different task performance in order to exhibit a learning effect on the HRF and compare our method to a state-of-the-art approach [9]. All experiments were performed in Python and our implementation along with the code for experimental validation is freely available online[1] in order to support reproducible research.

3.1. Results on synthetic data

Artificial time series. We randomly generated 100 neural activation signals $\boldsymbol{z}^*$ of 5 blocks, with an average duration of 12 s each and a standard deviation of 1 s. We choose a TR of 0.75s and a scan duration of 3 min to mimic the Human Connectome Project (HCP) protocol. We defined a common HRF shape $\boldsymbol{h}^*$ for all these artificial voxels. Last, we investigated 6 different scenarios with signal-to-noise-ratio (SNR) ranging from 1 to 20 dB.

Results. We tested our semi-blind deconvolution approach to recover the pair $(\widehat{\alpha}, \widehat{\boldsymbol{u}})$ from each measured time series and then deduce the HRF $\boldsymbol{h}_{\widehat{\alpha}}$ and the neural activation signal $\widehat{\boldsymbol{z}} = \boldsymbol{L}\widehat{\boldsymbol{u}}$. As shown in Fig. 1, in low SNR cases we did not perfectly recover both signals. In contrast, as the SNR increases the error of our estimator is significantly reduced by a factor of 3 on the most challenging problem (estimation of $\boldsymbol{z}$). A visual inpection of the different estimates confirms that our approach behaved accurately according to our model.

3.2. Results on real data

HCP Data. Our validation was performed on the HCP dataset [22] which comprises fMRI recordings of participants performing different motor tasks. The tasks were adapted from the protocol developed in [23]. We choose this dataset as it presented both a good temporal and spatial resolution. A short time of repetition (TR=720 ms) was actually used to collect interleaved simultaneous multislice echo-planar images with a Multi-Band factor of 8 and a spatial resolution of 2x2x2mm. Each fMRI run lasted 3min34s in total during which $n = 284$ scans were acquired. The fMRI data were already preprocessed using a classical pipeline including realignment, coregistration, spatial normalization and smoothing (5 mm isotropic). The EP was divided in two sets of motor tasks, with 15 s fixation blocks at the beginning, in the middle of the acquistion and at the end of the recording. Each task set was composed of 5 blocks of 12 s each, preceded by a 3 s cue indicating the task to be performed by the participant. The latter corresponded to moving the tongue, tapping the left or right finger or squeezing the left or right toes. In what follows, we only consider one participant even though our results are reproducible across individuals.

Voxel Selection. Each fMRI run comprises a huge data set consisting of 230,314 voxels (i.e. time series) recorded along 284 time points. As our method is so far univariate, it estimates an activation signal and HRF in each voxel independently. Hence, an important aspect in the validation consisted in selecting activated voxels for which these estimates are meaningful. Following the work in [9], we used a General Linear Model (GLM) that also embeds a supervised voxelwise HRF estimation to regress the convolution of the known EP with the HRF estimate on the measured BOLD signal. From all voxel candidates, we extracted the 100 mostly correlated which are associated with the highest coefficients in the GLM. This process is illustrated in Fig. 2.

Results. Fig. 3 presents the neural activation signals $\boldsymbol{z}$ estimated with our method for the left hand motor task in one participant. The estimated neural activation signals retrieved the two well defined blocks, suggesting that the model proposes coherent blocks for the neural activation signals with a timing close to that of the EP. Interestingly, one can observe that the measured BOLD signals are postponed in time as compared to the recovered neural activation signals, which is consistent with the sluggishness of the hemodynamic response.

[1] https://github.com/CherkaouiHamza/pybold

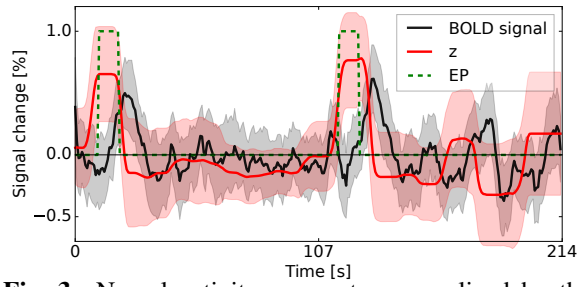

Fig. 3: Neural activity surrogates normalized by their ℓ_∞ norm. The standard deviation across voxels is encoded by transparency around mean curves for the EP (*green*), the pre-processed BOLD signals $\boldsymbol{y}$ (*black*) in the most correlated voxels, and the neural activation signals $\boldsymbol{z}$ (*red*) estimated with our semi-blind deconvolution approach for the same voxels.

Fig. 4 displays the HRF estimates for two tasks performed by the same participant using the method proposed in [9] and ours in the semi-blind deconvolution scheme. The HRF estimates were averaged across the 100 selected voxels. For the *visual fixation* task lasting 20 s in total, both methods recover a similar HRF shape. This was expected as the BOLD signal in response to the visual task elicits the strongest activity for both methods. The HRF curves depart from the canonical HRF as all the selected voxels did not confine to the primary visual system but were instead spread between motor and visual regions. For the *left hand motor* task lasting 24 s in total, the HRF shape recovered by the two approaches differ. The early initial dip found by [9] is questionable as such depletion may physiologically occur only in the first second after stimulation [24]. The HRF estimates obtained through semi-blind deconvolution appear more plausible even though the time-to-peak is quite large too. This difference is explained by the capacity of our model to cope with the latencies between the EP and the neural activity signal. Moreover, the HRF estimates obtained using [9] are close to each other. In contrast, Fig. 4 shows that our HRF estimate significantly differs from the one in response to the *left hand* task. This suggests a task-dependent shape for the HRF as previously demonstrated in the literature [6]. Moreover, when we used other tasks available in the HCP dataset we still noticed this coherent task-dependent or learning effect: for instance, the *right* and *left hand* tasks provide similar HRFs to the *right* and *left foot* tasks, respectively.

4. CONCLUSION

In this work, we recovered coherent HRF estimates in voxels correlated with a specific task without the explicit knowledge of the experimental paradigm. To do so, we simultaneously estimated a neural activation signal, which may depart from the EP in terms of timing. We observed a clear dependence between the HRF shape and the different tasks involved in the

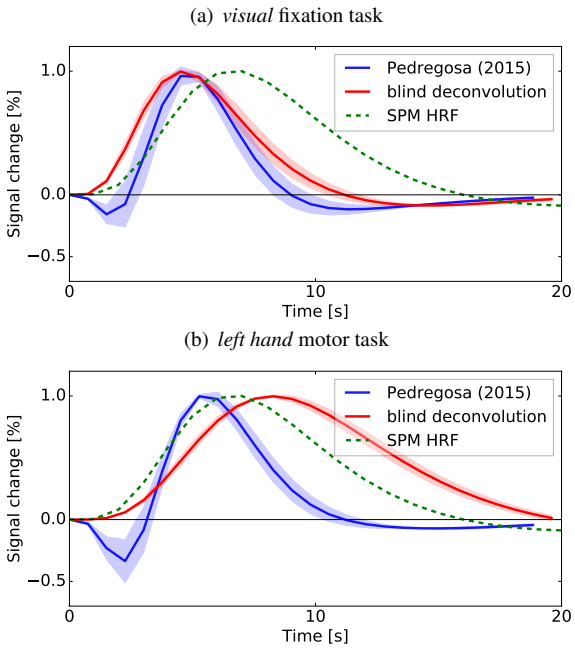

Fig. 4: HRF estimates computed for two different tasks in one participant to the HCP protocol. In (*green*) the canonical SPM HRF, in (*blue*) the reference HRFs estimated using [9] and in (*red*) the HRFs estimated using the proposed semi-blind deconvolution technique.

EP. For the first time in the fMRI literature, our approach performs an optimization-driven voxelwise semi-blind deconvolution scheme of the BOLD signal with a block neural activation signal. However, several limitations remain. The ℓ_1 norm regularization parameter λ gathers the statistical relevance of our model and is set by hand so far. Futur developement, such as a more robust deconvolution technique with a concomitant Lasso or the squared root Lasso could be explored. The dependence on the reference HRF should be investigated too. Moreover, the described method remains purely univariate and could be advantageously extented to a multivariate framework by aggregating the data to limit the number of unknown neural activation signals with rank-1 structure [25]. This contribution clearly opens new research avenues especially for inspecting functional connectivity between distant brain regions by cross-correlating pairs of neural activity signals instead of BOLD signals and therefore better disentangling vascular from neuronal effects.

Acknowledgment

This work was supported by the CEA PhD scholarship, the UK Royal Academy of Engineering under the Research Fellowship Scheme (RF/201718/17128), and the SRPe PECRE 1718/15 Award.

5. REFERENCES

[1] S. Ogawa, D. W. Tank, R. Menon, J. M. Ellerman, S. G. Kim, H. Merkle, and K. Ugurbil, "Intrinsic signal changes accompagnying sensory simulation: functional brain mapping and magnetic resonance imagine," Proc. Natl. Acad. Sci., 1992, vol. 89, pp. 5951–5955.

[2] P. A. Bandettini, A. Jesmanowicz, E. C. Wong, and J. S. Hyde, "Processing strategies for time-course data sets in functional MRI of the human brain," *Magnetic resonance in medicine*, vol. 30, no. 2, pp. 161–173, 1993.

[3] G. M. Boynton, S. A. Engel, G. H. Glover, and D. J. Heeger, "Linear systems analysis of functional magnetic resonance imaging in human V1," *Journal of Neuroscience*, vol. 16, no. 13, pp. 4207–4221, 1996.

[4] C. Goutte, F. A. Nielsen, and L. K. Hansen, "Modeling the haemodynamic response in fMRI using smooth FIR filters," *IEEE transactions on Medical Imaging*, vol. 19, pp. 1188–1201, 2000.

[5] G. Marrelec, H. Benali, P. Ciuciu, M. Pélégrini-Issac, and J.-B. Poline, "Robust Bayesian estimation of the hemodynamic response function in event-related BOLD MRI using basic physiological information," vol. 19, no. 1, pp. 1–17, 5 2003.

[6] P. Ciuciu, J.-B. Poline, G. Marrelec, J. Idier, C. Pallier, and H. Benali, "Unsupervised robust nonparametric estimation of the hemodynamic response function for any fMRI experiment," *IEEE transactions on Medical Imaging*, vol. 22, pp. 35–51, 2003.

[7] T. Vincent, T. Rissern, and P. Ciuciu, "Spatially adaptive mixture modeling for analysis of fMRI time series," *IEEE transactions on Medical Imaging*, vol. 29, pp. 59–74, 2010.

[8] L. Chaari, L. Forbes, T. Vincent, and P. Ciuciu, "Hemodynamic-informed parcellation of fmri data in a joint detection estimation framework," in *proceedings of International Conference on Medical Image Computing and Computer-Assisted Intervention*, 2012, vol. 15, pp. 180–188.

[9] F. Pedregosa, M. Eickenberg, P. Ciuciu, B. Thirion, and A. Gramfort, "Data-driven HRF estimation for encoding and decoding models," *NeuroImage*, pp. 209–220, 2015.

[10] K. J. Friston, O. Josephs, G. Rees, and R. Turner, "Nonlinear eventrelated responses in fMRI," *Magnetic Resonance in Medicine*, vol. 39, pp. 41–52, 1998.

[11] M. A. Lindquist and T. D. Wager, "Validity and power in hemodynamic response modeling: a comparison study and a new approach," *Humain brain mapping*, vol. 28, pp. 764–784, 2007.

[12] F. I. Karahanoglu, C. Caballero-Gaudes, F. Lazeyras, and D. Van De Ville, "Total activation: FMRI deconvolution through spatio-temporal regularization," *NeuroImage*, vol. 73, pp. 122–134, 2013.

[13] B. A. Olshausen and D. J. Field, "Sparse coding with an incomplete basis set: a strategy employed by V1," *Vision Research*, vol. 37, no. 23, pp. 3311–3325, 1997.

[14] K.R Sreenivasan, M. Havlicek, and G. Deshpande, "Nonparametric hemodynamic deconvolution of fmri using homomorphic filtering," IEEE Trans Med Imaging., 2015, vol. 34, pp. 1155–1163.

[15] S. Makni, P. Ciuciu, J. Idier, and J.-B. Poline, "Joint detection-estimation of brain activity in functional MRI: a multichannel deconvolution solution," *IEEE Transactions on Signal Processing*, vol. 53, no. 9, pp. 3488–3502, 9 2005.

[16] K.J. Friston, P. Fletcher, O. Josephs, A. Holmes, M.D Rugg, and R. Turner, "Event-related fMRI: characterizing differential responses.," *Neuroimage*, vol. 7, pp. 30–40, 1998.

[17] A. Beck and M. Teboulle, "A fast iterative shrinkage-thresholding algorithm for linear inverse problems," *SIAM journal on imaging sciences*, vol. 2, pp. 183202, 2009.

[18] J. Friedman, T. Hastie, H. Höfling, and R. Tibshirani, "Pathwise coordinate optimization," *The Annals of Applied Statistics*, vol. 1, no. 2, pp. 302–332, 2007.

[19] T. Moreau, L. Oudre, and N. Vayatis, "DICOD: Distributed Convolutional Sparse Coding," in *proceedings of International Conference on Machine Learning*, Stockohlm, Sweden, 2018.

[20] R. H. Byrd, P. Lu, and J. Nocedal., "A limited memory algorithm for bound constrained optimization," *SIAM Journal on Scientific and Statistical Computing*, vol. 16, pp. 1190–1208, 1995.

[21] E. Jones, T. Oliphant, P. Peterson, et al., "Scipy: Open source scientific tools for python," 2001–.

[22] D. C. Van Essen, S. M. Smith, D. M. Barch, T. E.J. Behrens, E. Yacoub, and K. Ugurbil, "The wu-minn Human Connectome Project: An overview," *NeuroImage*, vol. 80, pp. 62–79, 2013.

[23] B. T. Yeo, F. M. Krienen, J. Sepulcre, M. R. Sabuncu, D. Lashkari, M. Hollinshead, J. L. Roffman, J. W. Smoller, L. Zollei, J. R. Polimeni, B. Fischl, H. Liu, and R. L. Buckner, "The organization of the human cerebral cortex estimated by intrinsic functional connectivity," *Neurophysiol*, vol. 106, pp. 1125–1165, 2011.

[24] A. Frau-Pascual, F. Forbes, and P. Ciuciu, "Physiological models comparison for the analysis of asl fmri data," in *International Symposium on Biomedical Imaging*, 2015, vol. 12, pp. 1348–1351.

[25] T. Dupré La Tour, T. Moreau, M. Jas, and A. Gramfort, "Multivariate convolutional sparse coding for electromagnetic brain signals," in *Advances in Neural Information Processing System (NeurIPS)*, Montreal, Canada, Dec. 2018.